Supporting Information

Comparison of Uranium(VI) and Thorium(IV) Silicates Synthesized via Mixed Fluxes Techniques

Haijian Li [†,‡], Philip Kegler[†], Vladislav V. Klepov[§], Martina Klinkenberg[†], Dirk Bosbach[†], Evgeny V. Alekseev[†,‡,*]

[†]Institute of Energy and Climate Research (IEK-6), Forschungszentrum Jülich GmbH, 52428 Jülich, Germany

[‡]Institut für Kristallographie, RWTH Aachen University, 52066 Aachen, Germany

[§]Samara National Research University, 443086 Samara, Russia

**contact E-Mail: e.alekseev@fz-juelich.de*

Supporting information

Figure S1. Polyhedral and nodal representations of the SBUs extracted from all reported uranyl silicate compounds.

Figure S2. Crystals of $K_{14}(UO_2)_3Si_{10}O_{30}$ (left), and $K_2(UO_2)Si_2O_6$ (right).

Figure S3. Experimental (red) and calculated (black) PXRD patterns of $K_{14}(UO_2)_3Si_{10}O_{30}$.

Figure S4. EDS analysis for $K_{14}(UO_2)_3Si_{10}O_{30}$.

Table S1. Atom ratios of $K_{14}(UO_2)_3Si_{10}O_{30}$**.** (U is keep as 3)

Figure S5. EDS analysis for $K_2(UO_2)Si_2O_6$.

Table S2. Atom ratios of $K_2(UO_2)Si_2O_6$**.** (U is keep as 1)

Figure S6. EDS analysis for $K_2ThSi_2O_7$

Table S3. Atom ratio of $K_2ThSi_2O_7$**.** (Th is keep as 1)

Figure S7. EDS analysis for $K_2ThSi_3O_9$

Table S4. Atom ratios of $K_2ThSi_3O_9$. (Th is keep as 1)

Table S5. EDS results of $K_2ThSi_2O_7$ at 900 °C with increasing K_2CO_3 contents.

Figure S8. The Si−O−Si angle of open-branched chain $Si_{10}O_{30}$ (a) and unbranched chain Si_2O_6 (b) are labeled. Note that a Si−O−Si angle in $K_2(UO_2)Si_2O_6$ is 180°.

Figure S9. (a) Polyhedral presentation of the structure of $K_2Ca_4((UO_2)(Si_2O_7)_2)$[1] with a one-dimensional chain structure. (b,d) Structure of the 2D slab consisting of UO_6 polyhedra connected by Si_2O_7 disilicates along the *c*-axis and corresponding to anion topology present in $Na_9F_2(UO_2)(UO_2)_2(Si_2O_7)_2$.[2] (c,e) Structure of the $K_8(UO_2)_2(Si_2O_7)_2$ slab along the *c*-axis and corresponding to anion topology present in $K_8(K_5F)U_6Si_8O_{40}$.[3]

Figure S10. (a) Polyhedral presentation of the structure of $K_2ThSi_2O_7$ ($C2/c$) along the b axis. (b) Polyhedral presentation of the structure of $K_2ZrSi_2O_7$[4] ($P112_1/b$) along the c axis. (c) Polyhedral presentation of the structure of $Na_2ZrSi_2O_7$[5] (P-1) along the c axis. Yellow: Th octahedra in $K_2ThSi_2O_7$ and Zr octahedra in $K_2ZrSi_2O_7$ and $Na_2ZrSi_2O_7$. Green: SiO_4 tetrahedra. Blue: Na atoms. Mauve: K atoms.

Figure S11. Th−O−Si and Si−O−Si angles in the system of $A^+{}_2ThSi_3O_9$ (A^+ = K, Rb, and Cs) wadeite structures.

Table S6. Coordination environments of thorium in the reported thorium oxo-anion phases and corresponding to the ionic potential of anions.

Table S7. Determined Raman shift (cm^{-1}) and proposed band assignments for $K_2(UO_2)Si_2O_6$ and $K_{14}(UO_2)_3Si_{10}O_{30}$, respectively.

Table S8. Determined Raman shift (cm^{-1}) and proposed band assignments for $K_2ThSi_3O_9$ and $K_2ThSi_2O_7$, respectively.

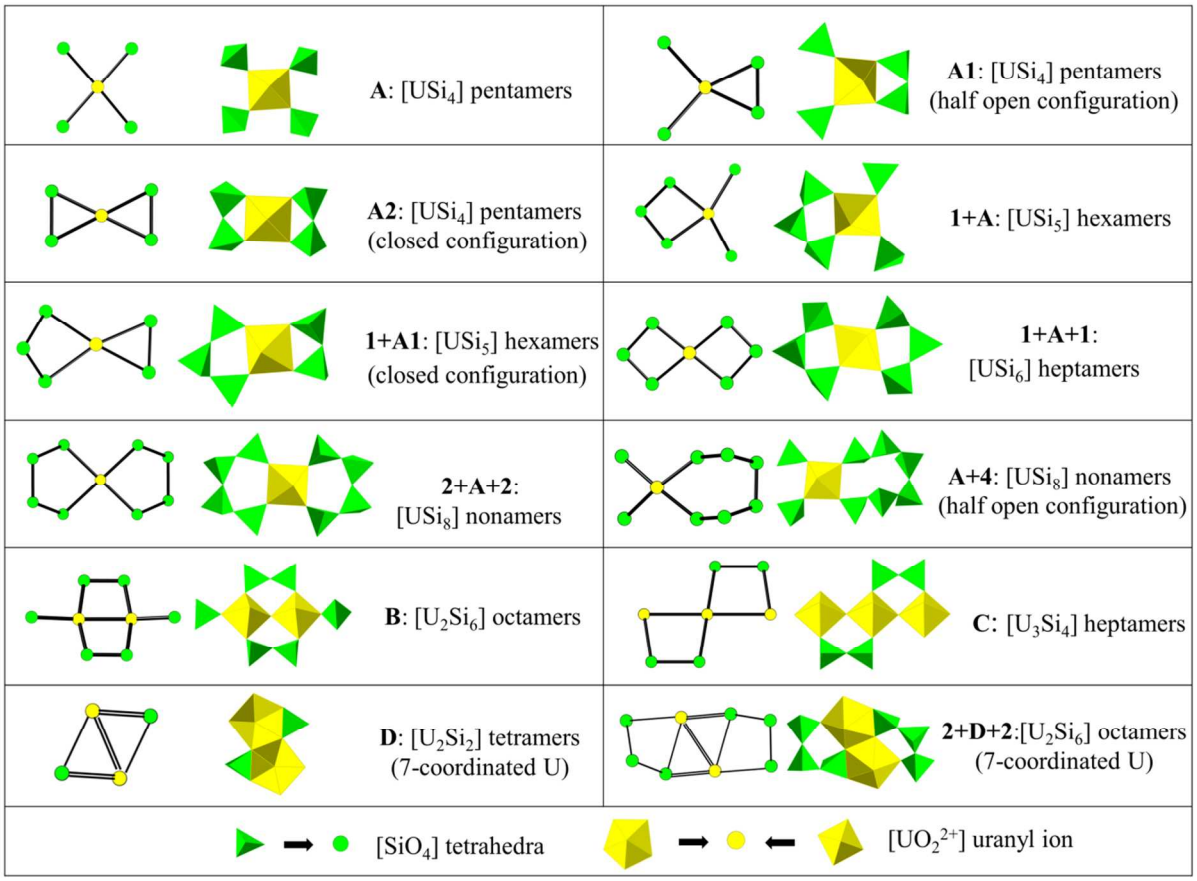

Figure S1. Polyhedral and nodal representations of the SBUs extracted from all reported uranyl silicate compounds.

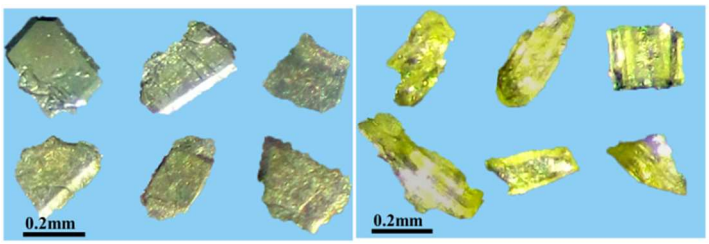

Figure S2. Crystals of $K_{14}(UO_2)_3Si_{10}O_{30}$ (left) and $K_2(UO_2)Si_2O_6$ (right).

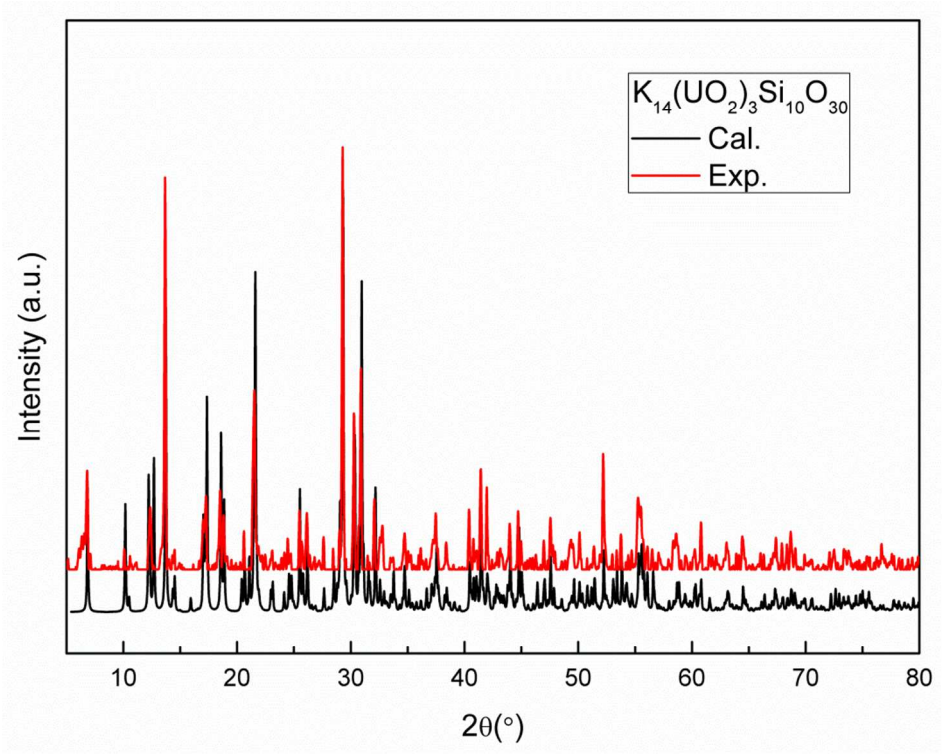

Figure S3. Experimental (red) and calculated (black) PXRD patterns of $K_{14}(UO_2)_3Si_{10}O_{30}$.

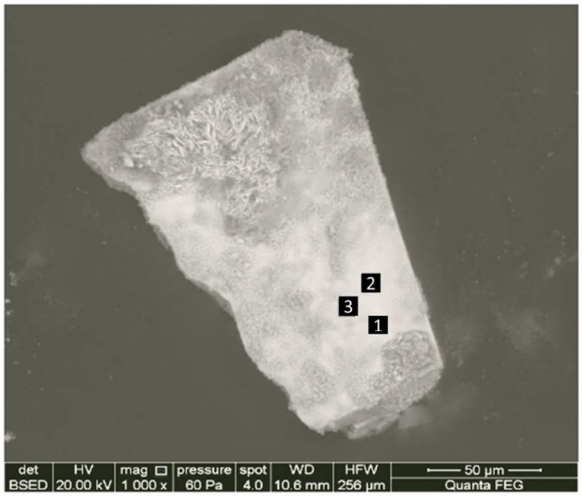

Figure S4. EDS analysis for $K_{14}(UO_2)_3Si_{10}O_{30}$

Table S1. Atom ratio of $K_{14}(UO_2)_3Si_{10}O_{30}$**.** (U is keep as 3)

	U	Si	K
Point1	3	12.93	13.97
Point2	3	12.47	13.00
Point3	3	12.60	14.06
Average	3	12.67	13.68

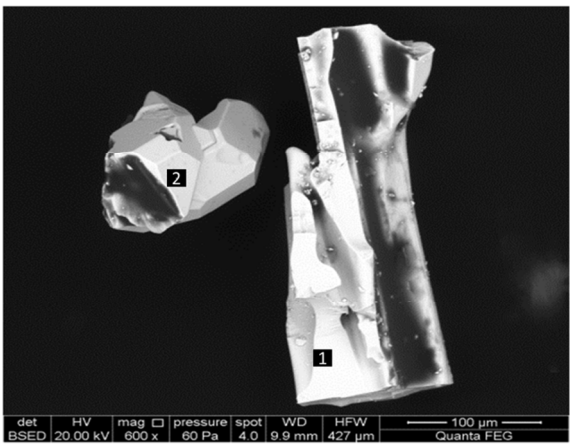

Figure S5. EDS analysis for $K_2(UO_2)Si_2O_6$

Table S2. Atom ratio of $K_2(UO_2)Si_2O_6$**.** (U is keep as 1)

	U	Si	K
Point1	1	2.07	2.04
Point2	1	2.92	1.88
Average	1	2.49	1.96

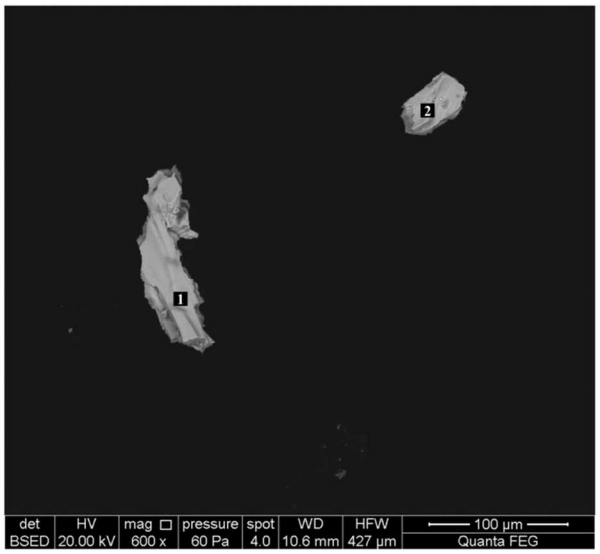

Figure S6. EDS analysis for $K_2ThSi_2O_7$

Table S3. Atom ratio of $K_2ThSi_2O_7$**.** (Th is keep as 1)

	Th	Si	K
Point1	1	2.05	2.01
Point2	1	2.42	1.88
Average	1	2.23	1.95

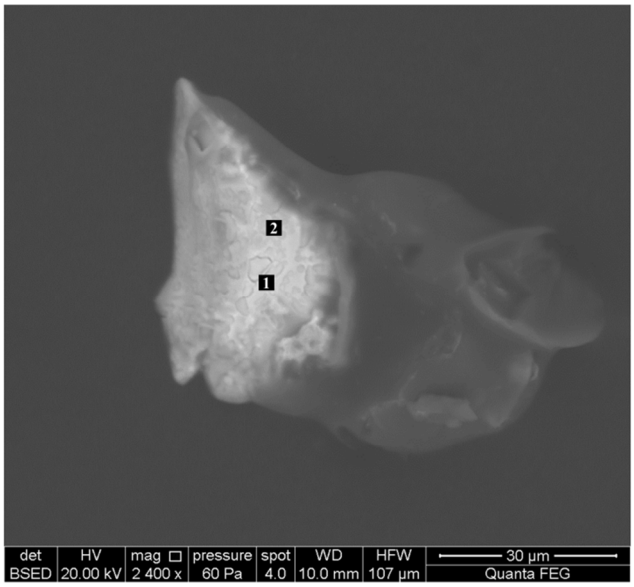

Figure S7. EDS analysis for $K_2ThSi_3O_9$

Table S4. Atom ratio of $K_2ThSi_3O_9$. (Th is keep as 1)

	Th	Si	K
Point1	1	3.61	1.75
Point2	1	3.37	1.85
Average	1	3.49	1.80

Table S5. EDS results of $K_2ThSi_2O_7$ at 900 °C with increasing K_2CO_3 contents.

Elements		Si (At%)	Th (At%)	K (At%)	O (At%)	Si/Th	K/Th
Original ratio	Spot 1	20.3	7.60	14.8	57.3	2.7	1.9
	Spot 2	19.4	14.3	12.5	53.9	1.4	0.9
150% K_2CO_3	Spot 1	20.0	8.2	15.1	56.7	2.5	1.8
	Spot 2	14.8	12.4	9.9	63.0	1.2	0.8
200% K_2CO_3	Spot 1	18.6	7.1	16.2	58.1	2.6	2.3
	Spot 2	18.9	11.9	16.2	53.0	1.6	1.4
250% K_2CO_3	Spot 1	19.3	18.6	17.0	45.0	1.0	0.9
	Spot 2	14.3	16.1	11.6	58.0	0.9	0.7
200% K_2CO_3 after washing	Spot 1	22.7	9.2	18.9	49.2	2.5	2.0
	Spot 2	19.2	12.0	15.7	53.1	1.6	1.3

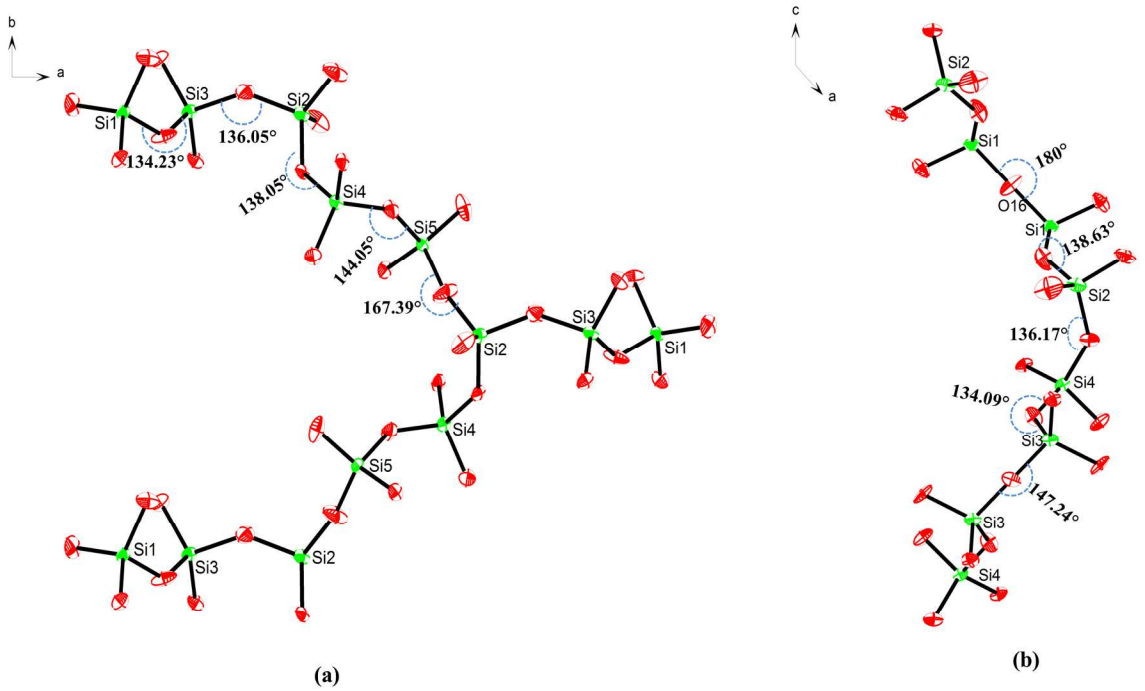

Figure S8. The Si−O−Si angle of open-branched chain $Si_{10}O_{30}$ (a) and unbranched chain Si_2O_6 (b) are labeled. Note that a Si−O−Si angle in $K_2(UO_2)Si_2O_6$ is 180°.

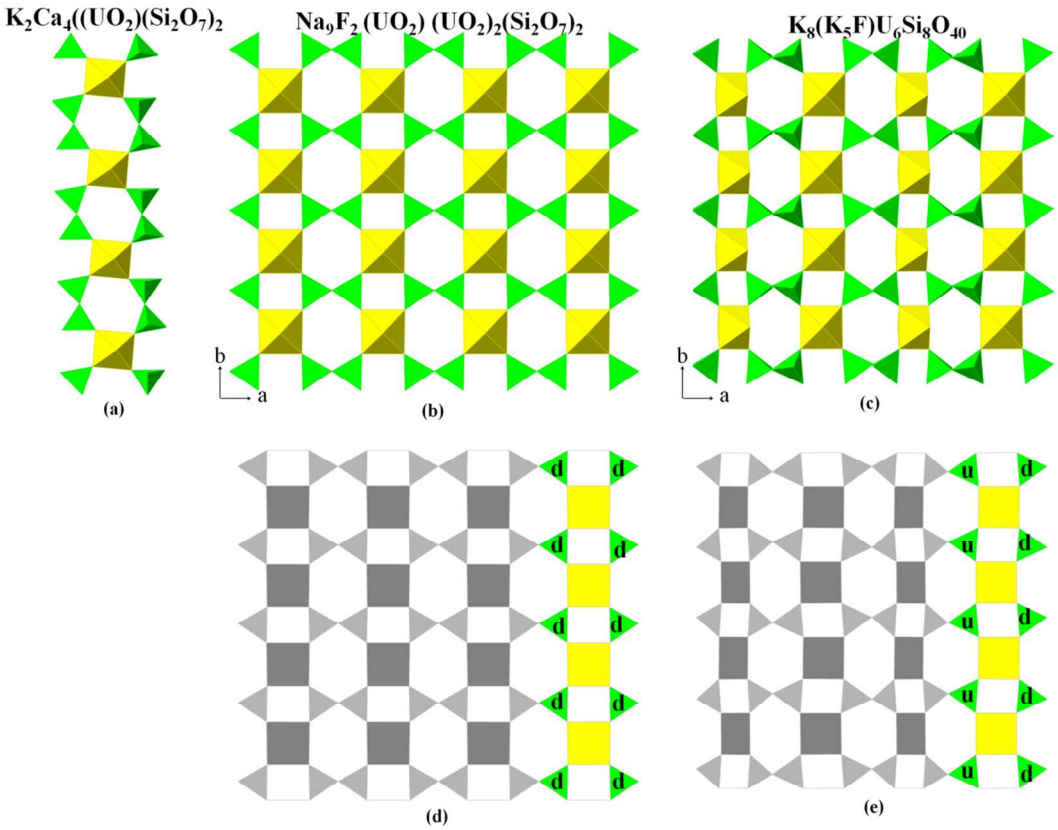

Figure S9. (a) Polyhedral presentation of the structure of $K_2Ca_4((UO_2)(Si_2O_7)_2)$[1] with a one-dimensional chain structure. (b,d) Structure of the 2D slab consisting of UO_6 polyhedra connected by Si_2O_7 disilicates along the *c*-axis and corresponding to anion topology present in $Na_9F_2(UO_2)(UO_2)_2(Si_2O_7)_2$.[2] (c,e) Structure of the $K_8(UO_2)_2(Si_2O_7)_2$ slab along the *c*-axis and corresponding to anion topology present in $K_8(K_5F)U_6Si_8O_{40}$.[3]

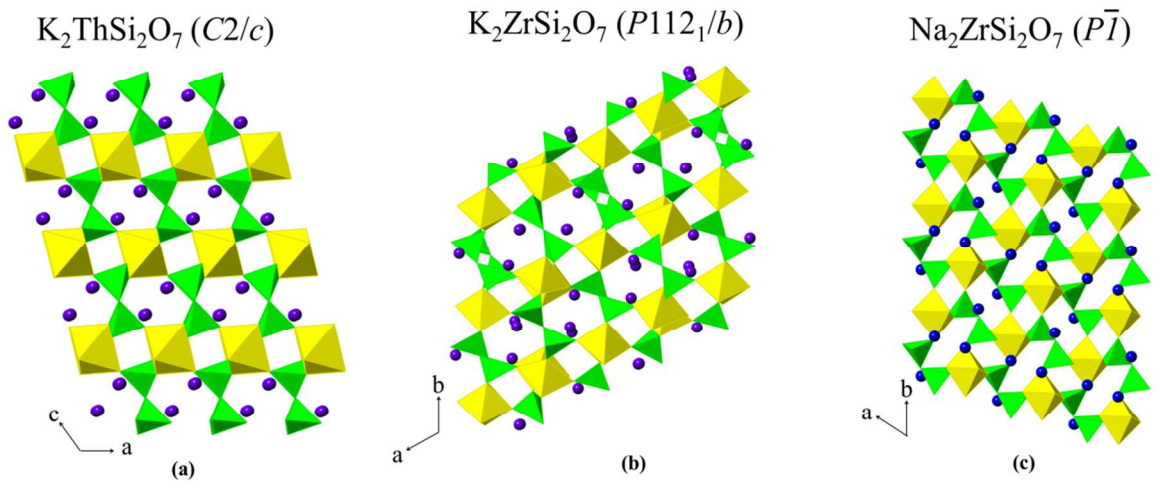

Figure S10. (a) Polyhedral presentation of the structure of $K_2ThSi_2O_7$ ($C2/c$) along the b axis. (b) Polyhedral presentation of the structure of $K_2ZrSi_2O_7$[4] ($P112_1/b$) along the c axis. (c) Polyhedral presentation of the structure of $Na_2ZrSi_2O_7$[5] (P-1) along the c axis. Yellow: Th octahedra in $K_2ThSi_2O_7$ and Zr octahedra in $K_2ZrSi_2O_7$ and $Na_2ZrSi_2O_7$. Green: SiO_4 tetrahedra. Blue: Na atoms. Mauve: K atoms.

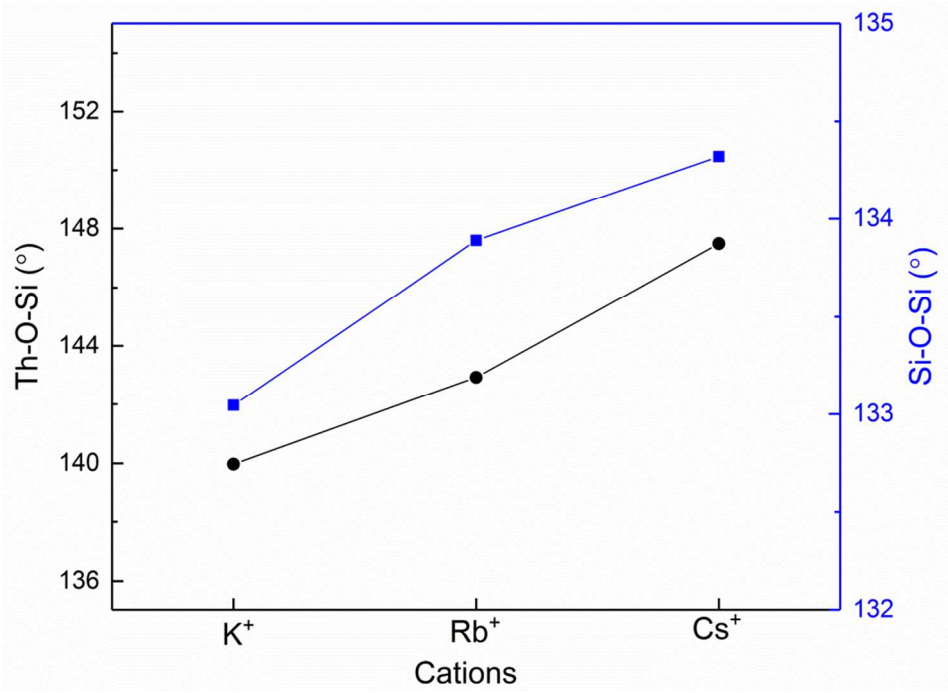

Figure S11. Th−O−Si and Si−O−Si angles in the system of $A^{+}_{2}ThSi_{3}O_{9}$ (A^{+} = K, Rb, and Cs) wadeite structures. The average values of Th−O−Si and Si−O−Si angles for $K_{2}ThSi_{3}O_{9}$ are given in the graph.

Table S6. Coordination environments of thorium in the reported thorium oxo-anion phases and corresponding to the ionic potential of anions.

Compounds	Coordination number (CN) of Th							Total	**Average of CN**	Anions	Radius of Anions (Å)	Valence	Ionic potential (IP)	**Average of IP**
	6	7	8	9	10	11	12							
Th-B-O			1	1	2		1	5	**9.8**	B +3	0.27	3	0.111	**0.111**
Th- Si/Ge -O	4	2	4	1		1		12	**7.5**	Si +4	0.40	4	0.1	**0.088**
										Ge +4	0.53	4	0.075	
Th- P/As-O	2	2	18	10	3	1		36	**8.36**	P +5	0.38	5	0.132	**0.120**
										As +5	0.46	5	0.109	
Th-Cr/Mo/W-O	2	2	18	14	1	1	1	38	**8.44**	Cr +6	0.44	6	0.136	**0.113**
										Mo +6	0.59	6	0.102	
										W +6	0.60	6	0.10	
Th-S/Se/Te -O			8	24	3			35	**8.86**	S +6	0.29	6	0.207	**0.152**
										Se +6	0.42	6	0.143	
										Te +6	0.56	6	0.107	

Table S7. Determined Raman shift (cm^{-1}) and proposed band assignments for $K_2(UO_2)Si_2O_6$ and $K_{14}(UO_2)_3Si_{10}O_{30}$, respectively.

$K_2(UO_2)Si_2O_6$	$K_{14}(UO_2)_3Si_{10}O_{30}$	Assignments	Ref.
276, 338	329	ν_2 $(UO_2)^{2+}$	6,7
	368	ν_3 $(SiO_4)^{4-}$	8
462	444, 460	ν_2 $(SiO_4)^{4-}$	6
	584	ν_4 $(SiO_4)^{4-}$	6
643	656	ν_4 $(SiO_4)^{4-}$	9
	680	ν_2 (Si–O–Si)	6
717, 730, 749	730, 738	ν_1 $(UO_2)^{2+}$	6
765		ν_1 (U-O bonds)	6
882	821, 845, 863	ν_1 $(UO_2)^{2+}$	6,10
932, 999	924	ν_1 $(SiO_4)^{4-}$	6,11
	1068	ν_3 $(SiO_4)^{4-}$	9

* ν_1 – symmetric stretching vibrations; ν_2 – symmetric bending vibrations; ν_3 – antisymmetric stretching vibrations; ν_4 – out of plane bending vibrations.

Table S8. Determined Raman shift (cm^{-1}) and proposed band assignments for $K_2ThSi_3O_9$ and $K_2ThSi_2O_7$, respectively.

$K_2ThSi_3O_9$	$K_2ThSi_2O_7$	Assignments	Ref.
	359	ν_3 $(SiO_4)^{4-}$	8
387	374	ν_2 $(SiO_4)^{4-}$	12
427	409	ν_2 $(SiO_4)^{4-}$	13
496	483	ν_2 $(SiO_4)^{4-}$	13
508	505	ν_2 $(SiO_4)^{4-}$	13
524	542	ν_2 $(SiO_4)^{4-}$	13
	570	ν_2 $(SiO_4)^{4-}$	13
623		ν_2 $(SiO_4)^{4-}$	13
716	694	ν_2 (Si–O–Si)	1,13
740		ν_2 $(SiO_4)^{4-}$	13
	790	ν_2 $(SiO_4)^{4-}$	13
858	834	ν_1 (Si–O)	12,14
	902	ν_1 (Si–O)	12,14
	911	ν_1 (Si–O)	12,14
923	923	ν_1 (Si–O)	12,14
	948	ν_1 (Si–O)	12,14
	967	ν_1 (Si–O)	12,14
	1007	ν_1 (Si–O)	12,14
1041	1044	ν_1 (Si–O)	12,14

* ν_1 – symmetric stretching vibrations; ν_2 – symmetric bending vibrations; ν_3 – antisymmetric stretching vibrations; ν_4 – out-of-plane bending vibrations.

REFERENCE

(1) Liu, C. L.; Liu, H. K.; Chang, W. J.; Lii, K. H. $K_2Ca_4[(UO_2)(Si_2O_7)_2]$: A Uranyl Silicate with a One-Dimensional Chain Structure. *Inorg. Chem.* **2015,** *54*, 8165-8167.

(2) Chang, Y. C.; Chang, W. J.; Boudin, S.; Lii, K. H. High-temperature, High-pressure Hydrothermal Synthesis and Characterization of A Salt-inclusion Mixed-valence Uranium(V,VI) Silicate: $[Na_9F_2][(U(V)O_2)(U(VI)O_2)_2(Si_2O_7)_2]$. *Inorg. Chem.* **2013,** *52*, 7230-7235.

(3) Morrison, G.; Tran, T. T.; Halasyamani, P. S.; zur Loye, H. C. $K_8(K_5F)U_6Si_8O_{40}$: An Intergrowth Uranyl Silicate. *Inorg. Chem.* **2016,** *55*, 3215-7.

(4) Chernov, A. N.; Maksimov, B. A.; Ilyukhin, V. V.; Belov, N. V. Crystalline Structure of Monoclinic Modification of K, Zr-Diorthosilicate-$K_2ZrSi_2O_7$. *Doklady Akademii Nauk Sssr.* **1970,** *193*, 1293-1296.

(5) Voronkov, A. A.; Shumyatskaya, N. G.; Pyatenko, Y. A. Crystal Structure of A New Natural Modification of $Na_2Zr(Si_2O_7)$. *J. Struct. Chem.* **1970,** *11*, 866–867.

(6) Frost, R. L.; Cejka, J.; Weier, M. L.; Martens, W. Molecular Structure of the Uranyl Silicates - a Raman Spectroscopic Study. *J. Raman Spectrosc.* **2006,** *37*, 538-551.

(7) Plesko, E. P.; Scheetz, B. E.; White, W. B. Infrared Vibrational Characterization and Synthesis of A Family of Hydrous Alkali Uranyl Silicates and Hydrous Uranyl Silicate Minerals. *Am. Mineral.* **1992,** *77*, 431-437.

(8) Amme, M.; Renker, B.; Schmid, B.; Feth, M. P.; Bertagnolli, H.; Dobelin, W. Raman Microspectrometric Identification of Corrosion Products Formed on UO_2 Nuclear Fuel During Leaching Experiments. *J. Nucl. Mater.* **2002,** *306*, 202-212.

(9) Chernorukov, N. G.; Kortikov, V. E. $Na[HSiUO_6]\cdot H_2O$: Synthesis, Structure, and Properties. *Radiochemistry* **2000,** *42*, 229–232.

(10) Xiao, B.; Schlenz, H.; Dellen, J.; Bosbach, D.; Suleimanov, E. V.; Alekseev, E. V. From Two-Dimensional Layers to Three-Dimensional Frameworks: Expanding the Structural Diversity of Uranyl Compounds by Cation-Cation Interactions. *Crystal Growth & Design* **2015,** *15*, 3775-3784.

(11) Matkovskii, A. O.; Gevorkyan, S. V.; Povarennykh, A. S.; Sidorenko, G. A.; Tarashchan, A. N. On the Bond Characteristics of UO in Uranyl Minerals from IR Spectroscopic Data. *Miner Sb Lvovskogo Gos Univ im Franko* **1979,** *33*, 11–22.

(12) Wierzbicka-Wieczorek, M.; Tobbens, D. M.; Kolitsch, U.; Tillmanns, E. Simultaneous Presence of $(Si_3O_{10})^{8-}$and $(Si_2O_7)^{6-}$ Groups in New Synthetic Mixed Sorosilicates: $BaY_4(Si_2O_7)(Si_3O_{10})$ and Isotypic Compounds, Studied by Single-crystal X-ray Diffraction, Raman Spectroscopy and DFT Calculations. *J. Solid State Chem.* **2013,** *207*, 94-104.

(13) Kahlenberga, V.; Kaindlb, R.; Többens, D. M. Z. Synthesis, Rietveld Analysis and Solid State Raman Spectroscopy of $K_4SrSi_3O_9$. *Anorg. Allg. Chem.* **2006,** *632*, 2037–2042.

(14) Kahlenberg, V.; Kaindl, R.; Sartory, B. On the existence of a second modification of $K_4SrSi_3O_9$ - X-ray single crystal diffraction, Raman spectroscopical and high temperature studies. *Solid State Sci.* **2007,** *9*, 65-71.